1-1-2020

Celastrol attenuates angiotensin II-induced cardiac remodeling by targeting STAT3

Shiju Ye
Wenzhou Medical University

Wu Luo
Wenzhou Medical University

Zia A. Khan
Wenzhou Medical University, zia.khan@schulich.uwo.ca

Gaojun Wu
Wenzhou Medical University

Lina Xuan
Harbin Medical University

See next page for additional authors

Circulation Research

ORIGINAL RESEARCH

Celastrol Attenuates Angiotensin II–Induced Cardiac Remodeling by Targeting STAT3

Shiju Ye,* Wu Luo,* Zia A. Khan,* Gaojun Wu, Lina Xuan, Peiren Shan, Ke Lin, Taiwei Chen, Jingying Wang, Xiang Hu, Shengjie Wang, Weijian Huang, Guang Liang

RATIONALE: Excessive Ang II (angiotensin II) levels lead to a profibrotic and hypertrophic milieu that produces deleterious remodeling and dysfunction in hypertension-associated heart failure. Agents that disrupt Ang II–induced cardiac dysfunction may have clinical utility in the treatment of hypertension-associated heart failure.

OBJECTIVE: We have examined the potential effect of celastrol—a bioactive compound derived from the Celastraceae family—on Ang II–induced cardiac dysfunction.

METHODS AND RESULTS: In rat primary cardiomyocytes and H9C2 (rat cardiomyocyte-like H9C2) cells, celastrol attenuates Ang II–induced cellular hypertrophy and fibrotic responses. Proteome microarrays, surface plasmon resonance, competitive binding assays, and molecular simulation were used to identify the molecular target of celastrol. Our data showed that celastrol directly binds to and inhibits STAT (signal transducer and activator of transcription)-3 phosphorylation and nuclear translocation. Functional tests demonstrated that the protection of celastrol is afforded through targeting STAT3. Overexpression of STAT3 dampens the effect of celastrol by partially rescuing STAT3 activity. Finally, we investigated the in vivo effect of celastrol treatment in mice challenged with Ang II and in the transverse aortic constriction model. We show that celastrol administration protected heart function in Ang II–challenged and transverse aortic constriction–challenged mice by inhibiting cardiac fibrosis and hypertrophy.

CONCLUSIONS: Our studies show that celastrol inhibits Ang II–induced cardiac dysfunction by inhibiting STAT3 activity.

VISUAL OVERVIEW: An online visual overview is available for this article.

Key Words: angiotensin II ■ heart failure ■ hypertension ■ molecular targeted therapy ■ signal transducer and activator of transcription 3

Meet the First Author, see p 944

Hypertension is the leading cause of heart failure and cardiovascular comorbidities in developed countries. Hypertensive heart disease is associated with adverse cardiac structural and functional remodeling, which ultimately leads to heart failure.[1] Diastolic dysfunction characterized by ventricular filling abnormalities is believed to represent an early and important pathophysiological step between hypertension and heart failure.[2] This is supported by the observation that nearly half of all patients with hypertension exhibit some evidence of diastolic dysfunction.[3] These functional deficits are brought upon by a plethora of factors, such as apoptosis of cardiomyocytes, adaptive ventricular remodeling, interstitial fibrosis, and disturbances in calcium handling.[4]

The role of the RAAS (renin-angiotensin-aldosterone system) in many cardiovascular disorders is well established. The octapeptide Ang II (angiotensin II) is the primary mediator of the RAAS system.[5] Studies have shown that Ang II induces an inflammatory phenotype in cardiomyocytes[6] and leads to cellular hypertrophy[7] and increased deposition of matrix proteins.[8] Furthermore, inhibiting Ang II has been shown to prevent cardiac

Correspondence to: Guang Liang, PhD, Department of Cardiology in the First Affiliated Hospital and School of Pharmaceutical Sciences, Wenzhou Medical University, Wenzhou 325035, China, Email wzmcliangguang@163.com; or Weijian Huang, MD, Department of Cardiology, the First Affiliated Hospital of Wenzhou Medical University, Wenzhou 325035, China, Email weijianhuang69@126.com

*S.Y., W.L., and Z.A.K. contributed equally to this article.

The Data Supplement is available with this article at https://www.ahajournals.org/doi/suppl/10.1161/CIRCRESAHA.119.315861.

For Sources of Funding and Disclosures, see page 1021.

Circulation Research is available at www.ahajournals.org/journal/res

Novelty and Significance

What Is Known?

- Angiotensin II induces an inflammatory phenotype in cardiomyocytes and leads to cellular hypertrophy and increased matrix protein deposition.
- Angiotensin II mediates cardiac injury, in part, through activating the JAK (janus kinase)/STAT (signal transducers and activators of transcription), downstream of AT1 (angiotensin type 1 receptor).
- Celastrol was shown to reduce cardiac fibrosis in experimental models of cardiac injury and failure.

What New Information Does This Article Contribute?

- Celastrol prevents Angiotensin II–induced cardiac hypertrophy and fibrosis by directly binding to and suppressing STAT3 tyrosine phosphorylation and nuclear translocation.
- Celastrol is effective in reducing the levels of activated STAT3, both before and after angiotensin II increase.
- Inhibitory activity of celastrol on STAT3 is independent of upstream signaling proteins, including AT1, JAK2, and other cytokine receptors.

In experimental models of cardiac failure, celastrol—a bioactive compound from *Celastrus orbiculatus*—has been shown to suppress fibrosis and hypertrophy. The exact underlying mechanisms, however, have not been defined. In this work, we identified the protein target of celastrol. We show that celastrol directly binds to and suppresses the activity of STAT3. Our studies implicate both SH2 (sarcoma gene homology domain) and coiled-coil domain of STAT3 as binding sites for celastrol, leading to reduced STAT3 tyrosine phosphorylation and nuclear translocation, respectively. Inhibition of STAT3 by celastrol also prevents the induction of STAT3 target genes including transforming growth factor-β1, collagen I, and myosin heavy chain. Finally, our studies show that celastrol prevents structural and functional deficits in both angiotensin II–induced and constrictive/occlusive models of cardiac failure, by targeting STAT3. Our data support the therapeutic potential of celastrol in targeting STAT3 for cardiac dysfunction and failure.

Nonstandard Abbreviations and Acronyms

β-MyHC	β-myosin heavy chain
Ang II	angiotensin II
AT1	Ang II receptor type 1
Bio-Celastrol	biotin-labeled celastrol
CCD	coiled-coil domain
Cy3-SA	Cy3-conjugated streptavidin
ERK	extracellular signal-regulated kinase
IL-1R	interleukin-1 receptor
IL-6	interleukin-6
JAK	janus kinase
KPNA3	importin-α3
PLC	phospholipase C
Prdx	peroxiredoxin
RAAS	renin-angiotensin-aldosterone system
rhSTAT3	recombinant human STAT3
S3I	S3I-201
STAT	signal transducer and activator of transcription
TAC	transverse aortic constriction
TGF-β1	transforming growth factor-β1

hypertrophy and fibrosis.[9] Adverse cardiac effects appear to be generated through AT1 (Ang II receptor type 1).[10] Recent studies show that AT1 receptor may activate JAK (janus kinase)/STAT (signal transducer and activator of transcription),[11] although the exact mechanism is unknown. Chronic activation of the STAT signaling pathway has been implicated in heart failure.[12] Therefore, detailed understanding of these mechanisms and agents regulating Ang II–induced alterations in the heart may prove to be clinically invaluble for the treatment of hypertensive heart failure.

Celastrol is a robust bioactive compound derived from *Tripterygium wilfordii*, *Celastrus orbiculatus*, and others that belong to the Celastraceae family.[13] Celastrol is widely used in China and other Asian countries for a number of indications, including chronic inflammatory and immunity disorders.[13] Although the mechanisms underlying these effects are not fully known, studies have shown involvement of nuclear factor-κB[14] and JAK/STAT pathway.[15] Recently, celastrol was shown to reduce cardiac fibrosis resulting from transverse aortic constriction (TAC) in mice.[16] Celastrol also inhibited cardiac fibrosis and infarct size in rats following permanent coronary artery occlusion.[17] Despite these promising results, the underlying mechanisms have not been identified. Furthermore, the activity of celastrol has not been tested in Ang II–induced cardiac remodeling.

In this study, we have investigated the effect of celastrol on Ang II–induced cardiomyocyte remodeling by utilizing H9C2 (rat cardiomyocyte-like H9C2) cells, as well as primary cardiomyocytes. We also challenged mice with Ang II to examine the protective effects of celastrol. Our studies show that celastrol prevents Ang II–induced

cardiomyocyte hypertrophy and matrix protein deposition. These findings were confirmed in mice challenged with Ang II, as well as in the TAC model. We have also discovered that celastrol provides these cardioprotective effects by binding to and inhibiting STAT3.

METHODS

Detailed experimental procedures, mouse models of cardiac dysfunction, and cell culture are described in Materials in the Data Supplement. Please see the Major Resources Table in the Data Supplement. Primers for real-time quantitative polymerase chain reaction (qPCR) assay are presented in Table I in the Data Supplement.

Data Availability

All other data are included within the article or the Data Supplement or available from the authors on request.

RESULTS

Celastrol attenuates Ang II–induced matrix protein production and hypertrophic remodeling in cardiomyocytes.

We exposed rat primary cardiomyocytes and H9C2 cells to Ang II and found elevated levels of hypertrophy marker[18] β-MyHC (β-myosin heavy chain; Figure 1A; Figure IA in the Data Supplement). These elevated levels remained for up to 36 hours. Based on a cell viability assay of celastrol at the 24-hour time point (Figure IB in the Data Supplement), we selected celastrol concentrations of 0.25, 0.5, and 1 nmol/L to assess its effects in cardiomyocytes. Ang II significantly increased the mRNA levels of β-MyHC, collagen I, and TGF-β1 (transforming growth factor-β1) in both primary cardiomyocytes and H9C2 cells, while pretreatment with celastrol inhibited Ang II–induced expression of these genes (Figure 1B; Figure IC in the Data Supplement). We also found that treatment with 1 nmol/L celastrol alone for 24 h did not change the levels of these proteins in H9C2 cells (Figure ID in the Data Supplement). Western blot assay showed dose-dependent inhibition of celastrol against Ang II–induced β-MyHC and TGF-β1 expression in primary cardiomyocytes (Figure 1C; Figure IE in the Data Supplement). Similar results were obtained in rat primary cardiac fibroblasts (Figure 1D; Figure IF in the Data Supplement). Furthermore, treatment of cells with celastrol 1 hour after exposure to Ang II also prevented the induction of β-MyHC, collagen I, TGF-β1, and TGF-β2 in primary cardiomyocytes (Figure IIA in the Data Supplement). Surprisingly, this reversal of hypertrophic changes by celastrol was seen even when celastrol was administered after 12 hours following exposure to Ang II (Figure IIB in the Data Supplement). These results show that cells preconditioned with celastrol or treated with celastrol after Ang II exposure respond similarly by reducing the levels of β-MyHC, collagen I, and TGF-β1.

To build on these findings, we performed rhodamine phalloidin staining of primary cardiomyocytes (Figure 1E; Figure IID in the Data Supplement) and H9C2 cells (Figure IIC and IIE in the Data Supplement) and show that celastrol decreases Ang II–induced cell size increase in cardiomyocytes. These results suggest that celastrol reduces Ang II–induced matrix protein expression and hypertrophy in cultured cardiomyocytes.

Identification of STAT3 as a Direct Celastrol-Binding Protein

To identify the molecular mechanism by which celastrol prevents Ang II–induced hypertrophy and fibrogenic gene expression, we screened for potential celastrol-binding proteins. To do this, we used biotin-labeled celastrol (Bio-Celastrol; Figure 2A) and assayed for the binding of celastrol to recombinant proteins fabricated on HuProt human protein microarray. Bio-Celastrol retains functional activity as can be seen by its inhibition of Ang II–induced fibrogenic gene expression in H9C2 cells (Figure III in the Data Supplement). Following Bio-Celastrol or free biotin incubation, binding was detected using Cy3-SA (Cy3-conjugated streptavidin; Figure 2B and 2C). We then calculated the signal-to-noise ratio, which was defined as the ratio of the foreground value and the background value. Cluster analysis was performed using the STRING software and showed that the celastrol preferably binds to Prdx (peroxiredoxin) proteins, Vps27-Hrs-STAM domain–containing proteins, and STAT proteins (Figure 2D). Transcriptome analysis showed that mRNAs of these 3 protein families are abundant in rat heart tissues, H9C2 cells, mouse heart tissues, and mouse cardiomyocytes (Figure IV in the Data Supplement).

Prdx are a ubiquitous family of cysteine-dependent peroxidase enzymes that regulate peroxide levels in cells.[19] Recent studies have shown robust expression of Prdx proteins in heart tissues, though their cardiac functions are poorly understood.[20] We, therefore, tested whether Prdx proteins are involved in Ang II–induced extracellular matrix production and hypertrophic changes in cardiac cells. We silenced Prdx1 and Prdx2 in H9C2 cells and primary cardiomyocytes and then challenged the cells with Ang II. Our results showed that Prdx1/2 knockdown did not alter Ang II–induced matrix protein production as well as the induction of β-MyHC (Figure V in the Data Supplement). These results suggest that Ang II–induced hypertrophic and fibrotic changes in the heart may be independent of Prdx alteration. The results also point to a Prdx-independent mechanism of the inhibitory activity of celastrol on Ang II–induced changes in cardiac cells.

Although Vps27-Hrs-STAM domain–containing proteins were also identified in our protein microarray assay, studies to date show that Vps27-Hrs-STAM proteins, such as Tom1 (target of Myb protein 1),

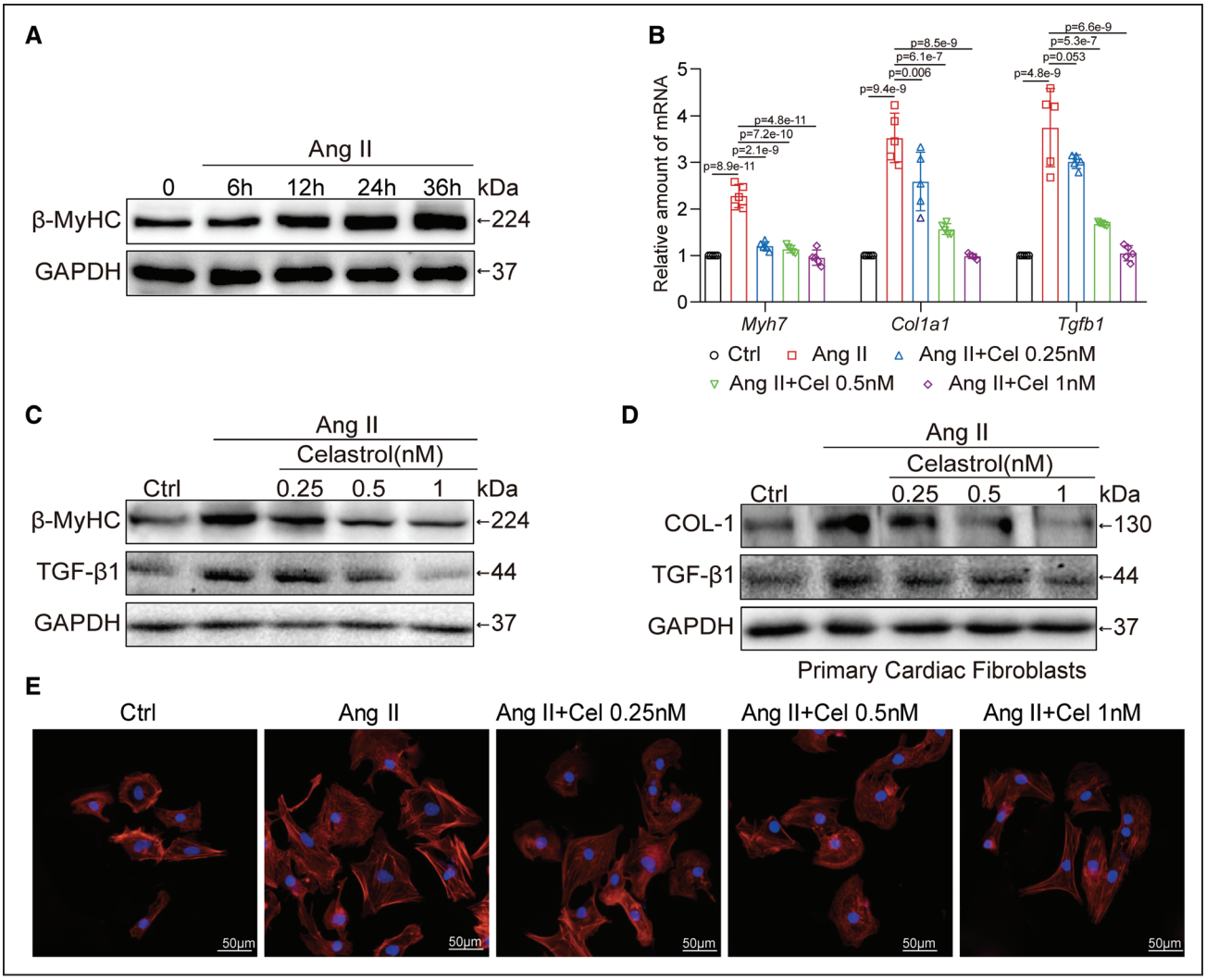

Figure 1. Celastrol attenuated Ang II (angiotensin II)–induced cardiomyocyte hypertrophy and fibrosis.
A, Time course of β-MyHC (β-myosin heavy chain) induction in response to Ang II in rat primary cardiomyocytes. Cells were exposed to 1 μmol/L Ang II for up to 36 h. Total proteins were extracted and subjected to analysis of β-MyHC protein levels. GAPDH was used as loading control. **B**, Real-time quantitative polymerase chain reaction analysis of β-MyHC, TGF-β1 (transforming growth factor-β1), and collagen-1 mRNA levels in primary cardiomyocytes. Cells were pretreated with celastrol or dimethyl sulfoxide (DMSO) vehicle for 1 h and then stimulated with 1 μmol/L Ang II for 6 h. **C** and **D**, Rat primary cardiomyocytes (**C**) and cardiac fibroblasts (**D**) were pretreated with increasing concentrations of celastrol (DMSO used as control) for 1 h and then stimulated with 1 μmol/L Ang II for 24 h. Cell lysates were probed for β-MyHC, collagen I, and TGF-β1 by Western blot analysis. GAPDH was used as loading control. **E**, Rhodamine phalloidin staining of primary cardiomyocytes showing the effect of celastrol on Ang II–induced hypertrophic responses. Cells were treated as in **C**. Slides were counterstained with DAPI (4',6-diamidino-2-phenylindole). **Lower Right**, Quantification of cell size ([**A**–**E**] n=5; 1-way ANOVA followed by Tukey post hoc tests [number of comparisons, 10]. Adjusted *P* values were provided in case of multiple groups).

Tom1L2 (TOM1-like protein 2), GGA1 (golgi-localized, gamma ear-containing, ARF-binding protein 1), GGA2 (golgi-localized, gamma ear-containing, ARF-binding protein 2), and HGS (hepatocyte growth factor-regulated tyrosine kinase substrate), function as adaptor proteins in regulating protein sorting in post-Golgi compartments.[21,22] There is also limited information on whether these proteins play a role in cardiac remodeling and in Ang II–induced cellular changes. However, of the potential celastrol-binding proteins, STAT3 piqued our interest as it has been shown to play a pivotal role in protecting cardiomyocytes[23,24] as well as mediating hypertrophy and remodeling upon abnormal activation.[25,26] In addition, STAT3 mRNA showed a higher level than STAT4 and STAT5 mRNAs in cardiac cells and rodent hearts (Figure IV in the Data Supplement). STAT3 binding in our assay also produced a robust signal-to-noise ratio of 3.95 (Figure 2E), suggesting that celastrol may mediate activities in cardiomyocytes by regulating STAT3. To validate the interaction of celastrol with STAT3 protein, we used surface plasmon resonance to evaluate the interaction at the molecular level. We observed that celastrol interacted with rhSTAT3 (recombinant human STAT3)

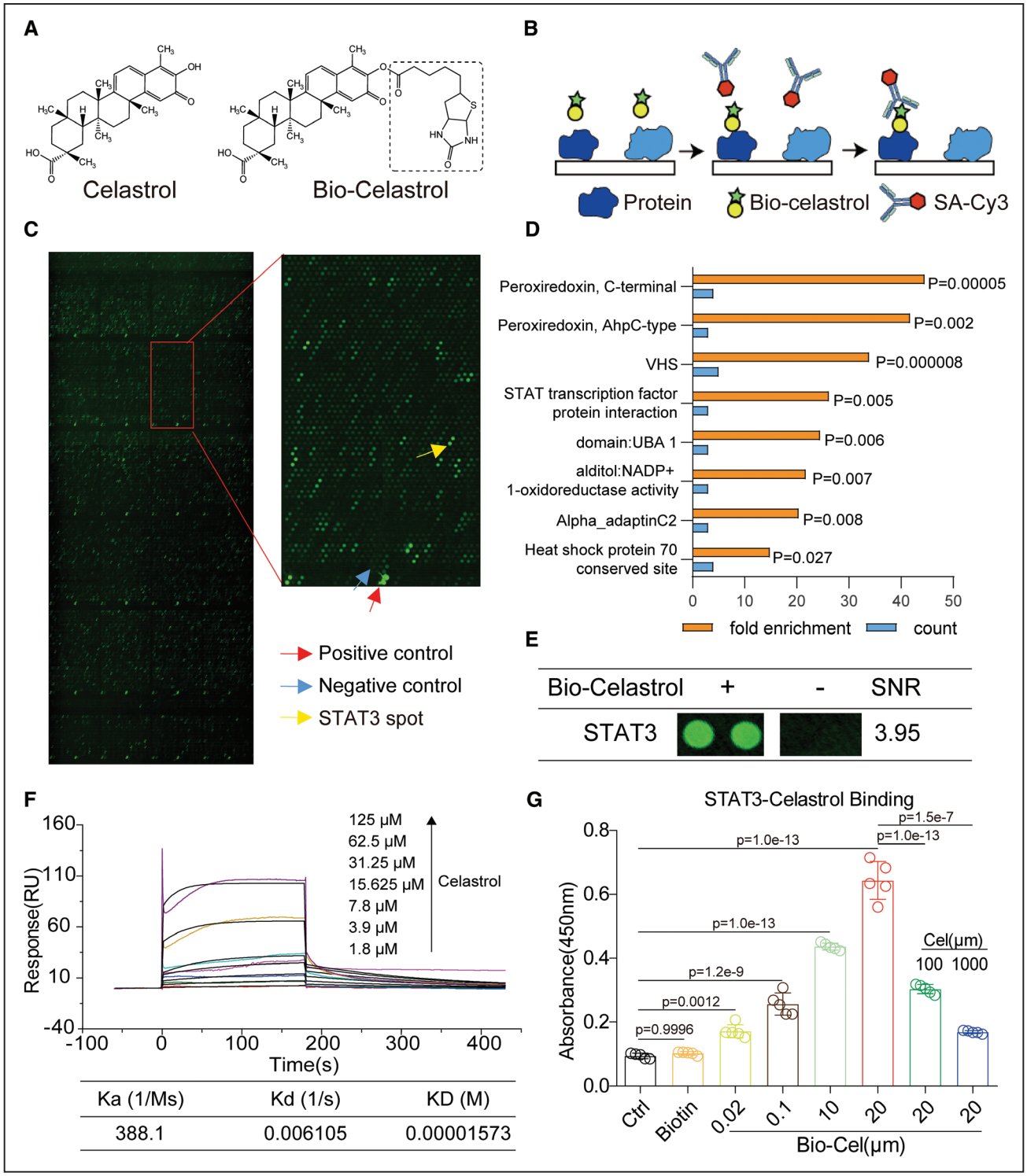

Figure 2. Identification of celastrol-binding proteins.
A, Chemical structure of celastrol and biotin-labeled celastrol (Bio-Celastrol). **B**, Schematic showing steps for identifying celastrol-binding proteins using microarrays fabricated with recombinant human proteins. **C**, Representative image of protein array showing positive (red arrow) and negative control (blue arrow) spots, as well as spots for STAT (signal transducers and activators of transcription)-3 (yellow arrow). **D**, Cluster analysis showing preferred binding partners of celastrol. Data show peroxiredoxin, Vps27-Hrs-STAM (VHS) domain–containing, and STAT protein families as top targets of celastrol. **E**, Magnified image of Bio-Celastrol binding to STAT3 spot on the protein array. Signal-to-noise ratio (SNR) is shown. **F**, Surface plasmon resonance (SPR) analysis showing direct interaction between celastrol and STAT3. Association and dissociation constants derived from data from 5 separate experiments (mean values shown). **G**, ELISA assay to determine celastrol binding to STAT3. rhSTAT3 (recombinant human STAT3) was captured by antibody coated on plates. Bio-Celastrol was then added at increasing concentrations. Label-free celastrol was added to determine whether it competes with the Bio-Celastrol (n=5; 1-way ANOVA followed by Tukey post hoc tests [number of comparisons, 28]. Adjusted *P* values were provided in case of multiple groups).

protein with a KD (the equilibrium dissociation constant) of 15.73 μmol/L (Figure 2F). To confirm this interaction, we used an ELISA-based system in which we captured rhSTAT3 and added Bio-Celastrol. Binding was then determined by streptavidin-horseradish peroxidase. Our results show that Bio-Celastrol interacts with rhSTAT3 and this interaction can be competitively inhibited by label-free celastrol (Figure 2G).

Binding Modes of Celastrol to STAT3 Protein

We then determined whether celastrol binds to STAT3 in cell and tissue lysates using biotinylated protein interaction pull-down assays. Bio-Celastrol was added to streptavidin-agarose beads, and lysates from H9C2 cells and mouse heart tissues were added. Our results show that Bio-Celastrol binds to STAT3 protein in lysates from both H9C2 cells and mouse heart tissues (Figure 3A and 3B). Interestingly, probing for upstream signaling proteins known to associate with STAT3, IL-1R (interleukin-1 receptor), and JAK2 did not show interaction with celastrol (Figure 3C). These results further validate that celastrol directly binds STAT3 but not upstream mediators.

To understand where in STAT3 protein celastrol may interact, we conducted a molecular docking and simulation study using the crystal structure of STAT3 (PDB:1BG1). The SH2 (sarcoma gene homology domain) domain and

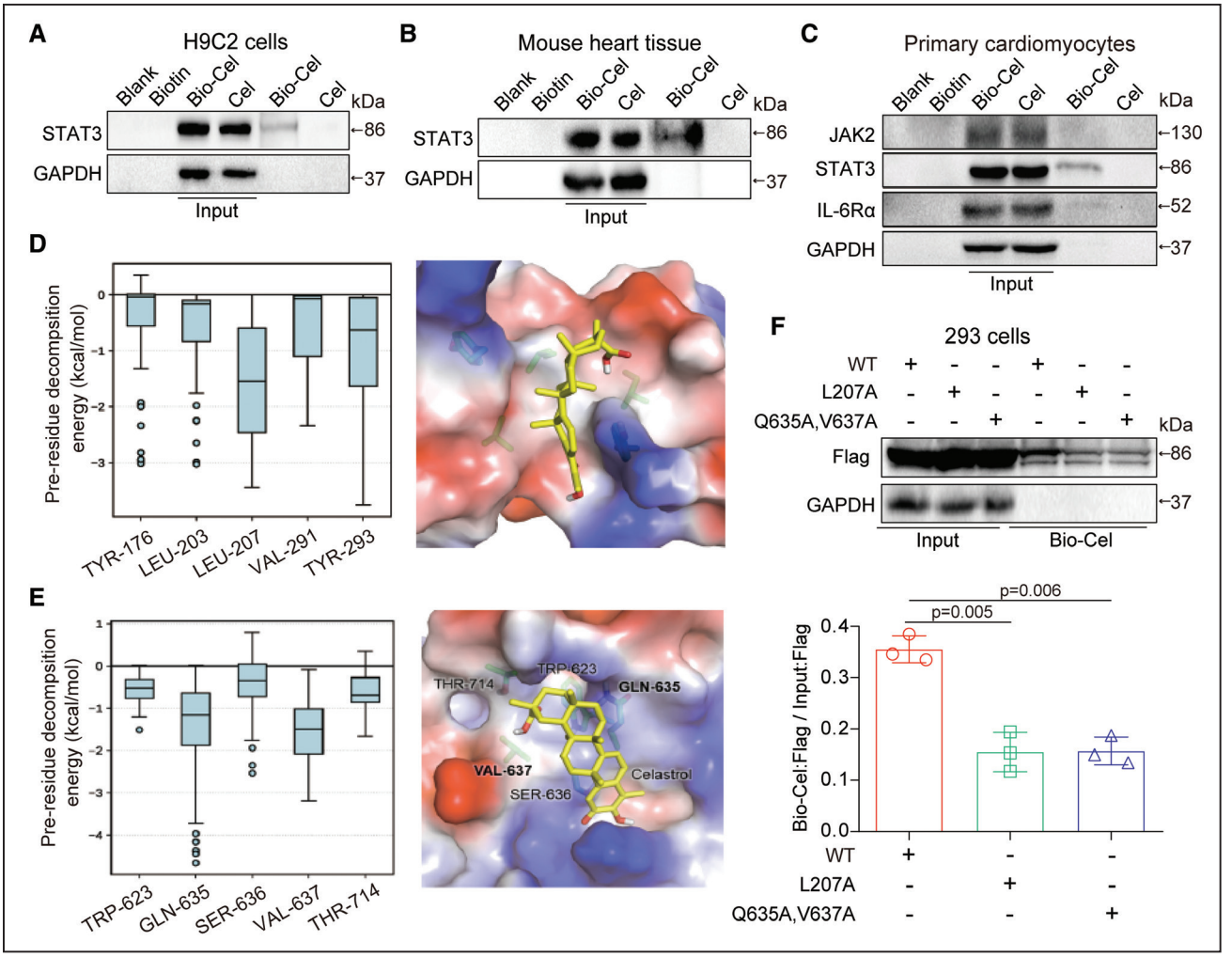

Figure 3. Celastrol binds STAT (signal transducers and activators of transcription)-3 protein.
A and **B**, biotinylated celastrol (Bio-Cel) was added to streptavidin-agarose beads and incubated. Biotin alone was used as a control. Lysates prepared from H9C2 (rat cardiomyocyte-like H9C2) cells (**A**) and mouse heart tissues (**B**) were added to the streptavidin-agarose beads with Bio-Cel. Eluent was then loaded on a polyacrylamide gel for Western blot analysis. Total lysates were used as an input control. **C**, Lysates prepared from primary cardiomyocytes were examined for celastrol binding to JAK (janus kinase)-2, STAT3, and IL6Rα (interleukin-6 receptor α) using pull-down assay described in **A**. **D** and **E**, Box plot of the per-residue decomposition energy of 5 key residues (**left**) and details of the binding pose of celastrol with the lowest binding energy (**right**) are shown for celastrol–coiled-coil domain (**D**) and celastrol-SH2 (sarcoma gene homology domain; **E**). The carbon atoms of 5 key residues side chain and celastrol are represented as transparent green sticks and yellow sticks, respectively. **F**, HEK-293 (human embryonic kidney 293) cells were transfected with WT (wild type) STAT3 or mutant STAT3 (L207A; Q635A/V637A, respectively). Lysates were added to pull-down assays to detect celastrol binding using pull-down assay described in **A**. **Right**, Densitometric quantification data (n=3; 1-way ANOVA followed by Tukey post hoc tests [number of comparisons, 3]. Adjusted *P* were provided in case of multiple groups).

coiled-coil domain (CCD) are 2 well-studied domains for designing or screening of STAT3 inhibitors.[27] SH2 domain of STAT3 binds to tyrosine phosphorylated cytokine receptors and phosphorylated tyrosine 705 in STAT3 homodimerization, while CCD domain is responsible for KPNA3 (importin-α3) interaction and nuclear translocation. Distributions of both docking scores and MM/GBSA (molecular mechanics/generalized born/surface area) scores show that celastrol may bind both domains of STAT3 (Figure VI in the Data Supplement). Greater negative scores are obtained in celastrol-SH2 domain interaction, indicating that celastrol has a higher binding affinity to SH2 domain compared with the CCD domain. To predict the binding position of celastrol on SH2 and CCD domains, a per-residue decomposition energy calculation was performed for the 100 docking poses. Five key residues in the CCD domain with the top-lowest average energy values are Tyr-176, Leu-203, Leu-207, Val-291, and Tyr-293 (Figure 3D). Among these, Leu-207 showed the lowest energy. For the SH2 domain, the 5 key residues with the top-lowest average energy values are Trp-623, Gln-635, Ser-636, Val-637, and Thr-714 (Figure 3E). Among these, Gln-635 and Val-637 appeared to be key residues based on the energy values.

We then mutated Leu-207 in the CCD domain and Gln-635/Val-637 in the SH2 domain to Ala to confirm their involvements in celastrol-STAT3 interaction. Three plasmids, wide-type pCMV3-flag-ratSTAT3, pCMV3-flag-ratSTAT3-L207A, and pCMV3-flag-ratSTAT3-Q635A/V637A, were constructed and transfected into HEK-293 (human embryonic kidney 293) cells. We determined whether Bio-Celastrol binds to mutated STAT3 in the transfected cells using biotinylated Celastrol pull-down assays. Our results show that Bio-Celastrol binds to wild-type STAT3-expressing 293 cell lysates, while significantly reduced binding was observed for HEK-293 cell lysates expressing mutant STAT3 (Figure 3F). These results suggest that Leu-207 in the CCD domain and Gln-635/Val-637 in the SH2 domain participate in celastrol-STAT3 interaction.

Celastrol Blocks Ang II–Induced STAT3 Activation in Cardiomyocytes

Binding of celastrol to STAT3 prompted us to examine whether celastrol inhibits Ang II–induced STAT3 activation and prevents cardiomyocyte remodeling by targeting STAT3. We probed for tyrosine 705–phosphorylated STAT3 proteins as a proxy for STAT3 activation. Recent studies have shown increased tyrosine 705 phosphorylation of STAT3 by Ang II in mesangial cells and cardiomyocytes.[28,29] Furthermore, various cytokines and growth factors activate STAT3 by Tyr-705 phosphorylation.[30] Our studies show that Ang II increases Tyr-705 phospho-STAT3 levels at 1 hour and reaches maximum level at 12 hours in primary cardiomyocytes (Figure 4A; Figure IXA in the Data Supplement). Ang II stimulation did not induce serine 727 phosphorylation of STAT3 in cardiomyocytes (Figure VIIA and VIIB in the Data Supplement). Although celastrol alone did not induce STAT3 Tyr-705 phosphorylation (Figure VIIC and VIID in the Data Supplement), pretreatment with celastrol prevented Ang II–induced STAT3 Tyr-705 phosphorylation in primary cardiomyocytes (Figure 4B; Figure IXB in the Data Supplement). Interestingly, celastrol reduced STAT3 phosphorylation even when administered following 8-hour exposure of cardiomyocytes to Ang II (Figure VIIIA and VIIIB in the Data Supplement).

We next determined whether celastrol is able to reduce phosphorylation of STAT3 initiated by other upstream mediators. We selected IL-6 (interleukin-6) and TGF-β1 for these studies. Exposure of primary cardiomyocytes to IL-6 and TGF-β1 increased STAT3 phosphorylation (Figure VIIIC and VIIID in the Data Supplement). Treatment of cells with celastrol reduced phosphorylated STAT3 levels in cardiomyocytes exposed to either IL-6 or TGF-β. This reduction in phosphorylated STAT3 was seen without changes to phospho-JAK2 (Figure VIIIE and VIIIF in the Data Supplement), indicating that celastrol targets STAT3 and not upstream JAK2.

As the key event in STAT3-mediated gene regulation is the nuclear translocation of STAT3, we measured STAT3 proteins in nuclear and cytosolic fractions. We show that celastrol reduces Ang II–mediated nuclear STAT3 translocation in primary cardiomyocytes (Figure 4C and 4D; Figure IXC and IXD in the Data Supplement). As expected, Ang II decreased cytosolic levels of STAT3, and this activity was also reversed by celastrol in a dose-dependent manner. An interesting finding was that celastrol reduced nuclear localization of STAT3, which may be unphosphorylated. Although it is believed that once STAT3 is activated, mainly through phosphorylation,[31] STAT3 forms dimers through reciprocal phosphotyrosine-SH2 domain interactions and translocates to the nucleus. It is possible, based on our data, that celastrol reduces STAT3 activity in cardiomyocytes at both the phosphorylation and nuclear translocation levels. Recently, studies have shown that KPNA3 could be the primary carrier for STAT3 nuclear import in cells.[32,33] Our docking simulations also indicate that celastrol may bind to the CCD of STAT3—a region that participates in KPNA3 interaction. Based on these observations, we tested the idea that celastrol binding to STAT3 may disrupt STAT3-KPNA3 association, which would reduce nuclear translocation. Our immunoprecipitation assay showed that Ang II increases STAT3-KPNA3 interaction, while this increased interaction was significantly inhibited by pretreatment with celastrol in primary cardiomyocytes (Figure 4E). Since celastrol-STAT3 interaction does not require tyrosine 705 phosphorylation (as evident in our in vitro/cell-free assays), these results suggest that

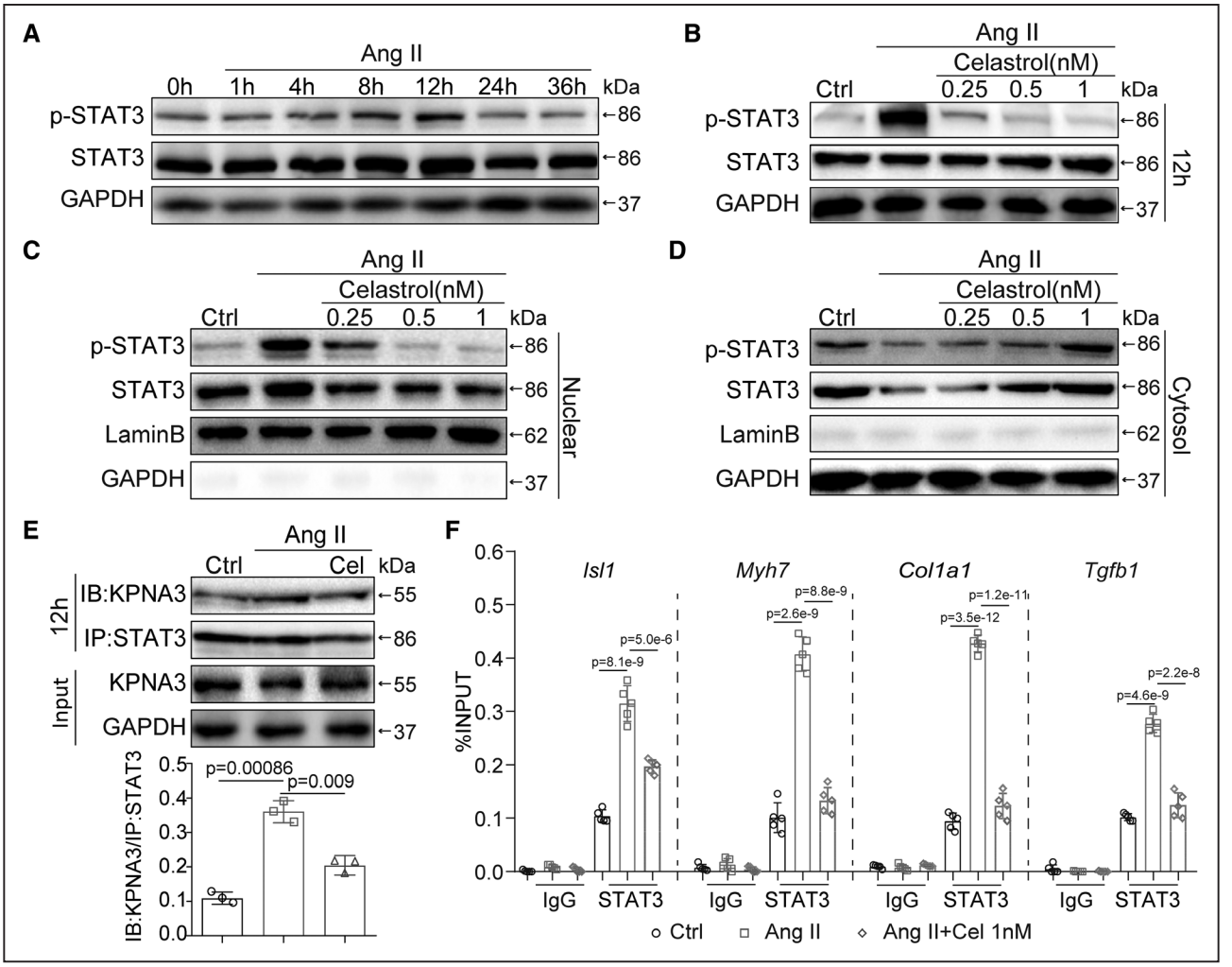

Figure 4. Celastrol inhibits Ang II (angiotensin II)–induced STAT (signal transducers and activators of transcription)-3 tyrosine 705 phosphorylation.

A, Rat primary cardiomyocytes were exposed to 1 μmol/L Ang II. Total proteins were isolated at different times and probed for phosphotylated STAT3 (p-STAT3) levels (Tyr-705). Total STAT3 and GAPDH were used as loading controls. **B**, Celastrol inhibits Ang II–induced STAT3 phosphorylation (Tyr-705). Primary cardiomyocytes were pretreated with celastrol for 1 h and then stimulated with 1 μmol/L Ang II for 12 h. Dimethyl sulfoxide (DMSO) was used as vehicle control. Total STAT3 and GAPDH were used for normalization. Whole cell lysates were used for Western blot assay. **C** and **D**, Celastrol inhibits Ang II–induced STAT3 nuclear translocation. Primary cardiomyocytes were pretreated with celastrol for 1 h and then stimulated with 1 μmol/L Ang II for 12 hours. Nuclear (**C**) and cytosolic (**D**) fractions were extracted and probed for p-STAT3/STAT3. Lamin B and GAPDH were used as loading controls. **E**, Celastrol inhibits Ang II–induced STAT3-KPNA3 (importin-α3) interaction. Primary cardiomyocytes were treated with 1 nmol/L celastrol for 1 h before exposure to 1 μmol/L Ang II for 12 h. KPNA3-STAT3 interactions were analyzed by coimmunoprecipitation. **Bottom**, Densitometric quantification. **F**, Chromatin immunoprecipitation-quantitative polymerase chain reaction analysis of STAT3 binding to candidate genes. Rat primary cardiomyocytes were treated as in panels above. ISL-1 (insulin gene enhancer protein) was used as positive control (**A**–**D** and **F**, n=5; **E**, n=5; **A**–**F**, 1-way ANOVA followed by Tukey post hoc tests [**A**: number of comparisons, 21; **B**–**D**: number of comparisons, 10; **E** and **F**: number of comparisons, 3]. Adjusted *P* values were provided in case of multiple groups).

celastrol may also regulate STAT3 nuclear localization, independent of its phosphorylation.

To determine the functional significance of nuclear STAT3, we examined whether STAT3 directly binds to the promoter regions of prohypertrophic and profibrotic genes to enhance the expression. To test this, we performed chromatin immunoprecipitation qPCR and show increased STAT3 binding at *ISL-1* (a positive control gene for STAT3), *myh7*, *Col1a*, *and Tgfb1* genes in Ang II–challenged primary cardiomyocytes (Figure 4F). This Ang II–induced STAT3 binding was prevented in cells pretreated with celastrol (Figure 4F). Thus, it is possible that celastrol prevents Ang II–induced prohypertrophic and profibrotic gene expression and cardiomyocyte remodeling by directly targeting STAT3.

Celastrol Attenuates Ang II–Induced Cardiomyocyte Remodeling by Targeting STAT3

We transfected primary cardiomyocytes with STAT3-targeting siRNA and STAT3-expressing plasmids. Knockdown of STAT3 (Figure 5A) inhibited Ang II–induced

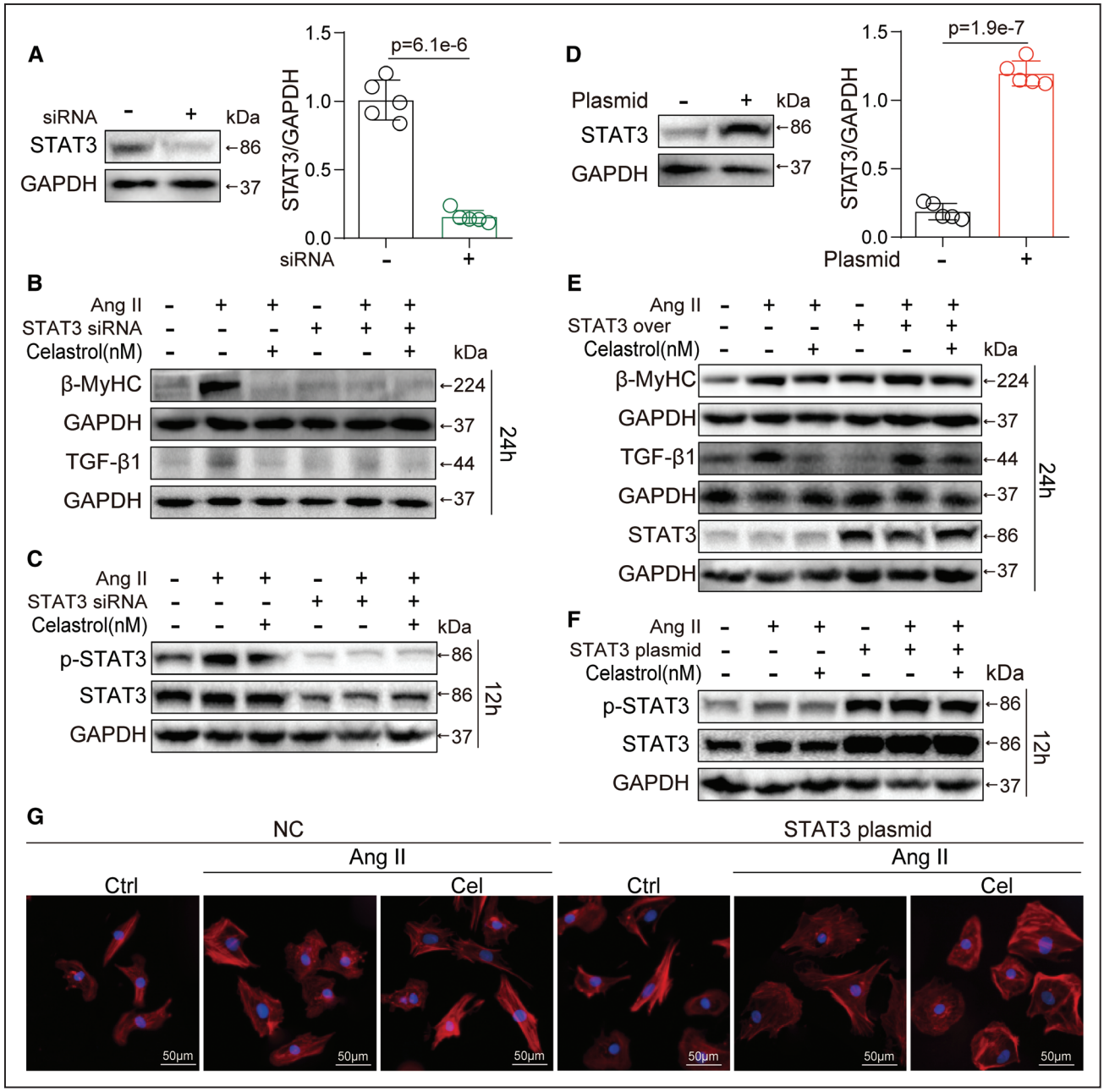

Figure 5. Involvement of STAT (signal transducers and activators of transcription)-3 in celastrol-mediated cardiomyocyte protection.

A, Primary cardiomyocytes were transfected with siRNA against STAT3. Control cells were transfected with negative control siRNA. Western blot was used to determine knockdown efficiency. Quantification is shown on **right**. **B**, Immunoblot analysis of β-MyHC (β-myosin heavy chain) and TGF-β1 (transforming growth factor-β1) following STAT3 knockdown. Primary cardiomyocytes transfected with negative control or STAT3 siRNA were treated with celastrol for 1 h and then exposed to Ang II (angiotensin II) for 24 h. GAPDH used as loading control. **C**, Immunoblot analysis of tyrosine 705–phosphorylated STAT3 following STAT3 knockdown in primary cardiomyocytes. Total STAT3 and GAPDH used as control. **D**, Primary cardiomyocytes were transfected with cDNA plasmids encoding STAT3. Control cells were transfected with empty vector. Western blot was used to determine STAT3 expression. Quantification is shown on right. **E**, Effect of STAT3 overexpression on β-MyHC and TGF-β1 induction by Ang II. Transfected Primary cardiomyocytes were treated as in **B**. **F**, phosphotylated STAT3 (p-STAT3) levels in primary cardiomyocytes following STAT3 overexpression. Total STAT3 and GAPDH used as control. **G**, Rhodamine/phalloidin staining of STAT3-overexpressing primary cardiomyocytes. Cells transfected with STAT3 or empty plasmid (negative control [NC]) were treated as in **D**. Slides were counterstained with DAPI (4′,6-diamidino-2-phenylindole; **A**–**G**, n=5; **A** and **D**, Student *t* test; **C**–**G**, 1-way ANOVA followed by Tukey post hoc tests [**C**–**G**: number of comparisons, 15]. Adjusted *P* were provided in case of multiple groups).

hypertrophic (β-MyHC) and profibrotic (TGF-β1) markers (Figure 5B; Figure IXE and IXF in the Data Supplement). This inhibition of hypertrophic and fibrotic factors in cells with STAT3 knockdown was associated with reduced STAT3 tyrosine 705 phosphorylation (Figure 5C; Figure IXG in the Data Supplement). We did

not see a significant potentiation effect on β-MyHC and TGF-β1 levels when STAT3 siRNA-transfected cells were treated with celastrol before Ang II exposure. Perhaps, this is because the knockdown was not robust enough. Conversely, however, overexpression of STAT3 (Figure 5D) alone did not increase β-MyHC and TGF-β1 levels in H9C2 cells (Figure 5E; Figure IXH and IXI in the Data Supplement) but did produce higher phosphorylated STAT3 proteins (Figure 5F; Figure IXJ in the Data Supplement). In this saturating condition, celastrol failed to reduce the levels of β-MyHC and TGF-β1 proteins and phosphorylated STAT3 in STAT3-overexpressing cells (Figure 5E and 5F; Figure IXJ and IXK in the Data Supplement). Rhodamine phalloidin staining of cardiomyocytes confirmed that STAT3 overexpression prevents the inhibitory activity of celastrol on cell hypertrophy (Figure 5G; Figure IXL in the Data Supplement). Collectively, these results suggest that celastrol engages STAT3 in inhibiting Ang II–induced cardiomyocyte remodeling.

We know that once Ang II binds to AT1, both G protein–dependent and independent signaling pathways are activated. G protein activation of PLC (phospholipase C) acts to increase protein kinase C. Binding of β-arrestin1 to AT1 inhibits G protein coupling and downstream activation of cytoplasmic ERK (extracellular signal-regulated kinase). In addition, AT1 induces the activation of JAK/STAT pathway. To explore how Ang II mediates STAT3 activation and possible node of inhibition by celastrol, we knocked down the expression of AT1 receptor in primary cardiomyocytes (Figure XA in the Data Supplement) and show that Ang II–induced JAK2 and STAT3 phosphorylation is reduced (Figure XB in the Data Supplement). These results show that Ang II employs AT1 to activate JAK/STAT pathway. We then used 2 biased activators of AT1: TRV027 and TRV055. TRV027 is a potent synthetic β-arrestin1–biased ligand[34] for AT1, whereas TRV055 selectively activates the PLCβ pathway downstream of AT1.[35] Our results show that both TRV027 and TRV055 failed to increase phosphorylated JAK2 and STAT3 Figure XC in the Data Supplement). This indicates that Ang II–induced STAT3 activation in cardiomyocytes is mediated through AT1 but is independent of β-arrestin1 and PLCβ. We confirmed this notion by silencing β-arrestin1 in cardiomyocytes before exposing the cells to Ang II (Figure XD in the Data Supplement). We show that β-arrestin1 knockdown does not suppress Ang II–induced JAK/STAT activation (Figure XE in the Data Supplement). To build on these results, we treated Ang II–exposed cells to celastrol and measured AT1-arrestin complex formation and phosphorylation of ERK and PLCβ. We show that celastrol does not alter Ang II–induced AT1–β-arrestin1 complex formation (Figure XF in the Data Supplement) or activation of ERK (Figure XG in the Data Supplement) and PLCβ (Figure XH in the Data Supplement). These results suggest that celastrol carries out its inhibitory activity by directly targeting STAT3, downstream of AT1.

Administration of Celastrol Reduces Ang II–Induced Cardiac Dysfunction and Remodeling

Our next objective was to determine whether celastrol inhibits Ang II–induced STAT3 activation and cardiac remodeling in mice. We used a mouse model with continuous Ang II infusion by subcutaneous osmotic mini pumps (Table 1).[36] This continuous Ang II delivery model shows cardiac fibrosis and hypertrophy, but ejection fraction (%) and fractional shortening (%) are preserved[36] or enhanced.[37,38] A selective

Table 1. Biometric and Echocardiographic Measurements in Experimental Mice: Model 1

	Ctrl	Cel (1 mg/kg)	Continuous Ang II Pump Infusion		
				Cel (1 mg/kg)	S3I (5 mg/kg)
	n=7	n=7	n=7	n=7	n=7
EF, %	78.97±1.18	78.58±0.71^{ns}	83.03±1.33*	78.87±1.28#	78.18±1.03#
FS, %	40.73±1.84	40.67±0.59^{ns}	45.14±1.4*	40.34±1.01#	40.42±0.76#
LVIDd, mm	2.12±0.12	2.17±0.16^{ns}	1.85±0.07*	2.17±0.11#	2.15±0.17 #
IVSD, mm	0.91±0.03	0.92±0.02^{ns}	0.94±0.02*	0.92±0.02#	0.92±0.17#
PWd, mm	0.69±0.02	0.71±0.03^{ns}	0.72±0.02*	0.70±0.14^{ns}	0.72±0.02^{ns}
E wave, m/s	0.68±0.08	0.63±0.15^{ns}	0.60±0.08*	0.65±0.08^{ns}	0.66±0.11^{ns}
Tei Index	0.83±0.14	0.82±0.028^{ns}	0.85±0.19^{ns}	0.84±0.15^{ns}	0.83±0.32#
IRT, ms	15.67±0.56	17.3±0.92^{ns}	12.83±0.73*	16.71±0.92^{ns}	17.42±1.36^{ns}
HW/BW, mg/g	5.55±0.26	5.59±0.16^{ns}	6.83±0.53*	5.65±0.35#	5.68±0.28#

Transthoracic echocardiography was performed on mice at the end of the animal study. Data presented as mean±SEM (n=7; 1-way ANOVA followed by Tukey post hoc tests; number of comparisons, 10). Ang II indicates angiotensin II; BW, body weight; Cel, celastrol; Ctrl, control; EF ejection fraction; FS, fractional shortening; HW, heart weight; IRT, isovolumic relaxation time; IVSD, diastole interventricular septal thickness; LVIDd, diastole left ventricle internal dimension; ns, no significance; PWd, diastole posterior wall thickness; S3I, S3I-201; and Tei index, a myocardial performance index designed by Dr Chuwa Tei.

*$P<0.05$ compared with Ctrl.

#$P<0.05$ compared with Ang II.

STAT3 inhibitor S3I-201 (S3I)[39] was used as a positive control to determine whether celastrol activity can be mimicked by STAT3 inhibition. As shown in Figure XIA in the Data Supplement, Ang II infusion caused an increase in Ang II levels in heart tissues of mice. Treatment of mice with STAT3 inhibitor S3I and celastrol did not alter cardiac Ang II levels. In addition, mice showed significantly increased systolic blood pressure upon Ang II challenge (Figure XIB in the Data Supplement). Neither celastrol nor S3I suppressed Ang II–induced blood pressure, which is consistent with the in vitro data that celastrol did not affect Ang II–induced AT1–β-arrestin1 interaction and ERK/PLCβ phosphorylation (Figure XF through XH in the Data Supplement). Furthermore, no changes in body weights were noted among any of the experimental groups (Figure XIC in the Data Supplement).

Cardiac function in mice was determined by noninvasive echocardiography (Figure XID in the Data Supplement). As shown in Table 1, Ang II challenge increased ejection fraction (%) and fractional shortening (%), while left ventricular internal dimension in diastole and E wave were decreased. Previous studies have shown that low-dose continuous Ang II infusion for 2 weeks increases ejection fraction (%) and fractional shortening (%),[37,38] possibly as a compensatory mechanism. Heart weights of mice were also increased indicating hypertrophic changes. These alterations were normalized by celastrol and S3I. These results indicated that STAT3 inhibitor and celastrol attenuated Ang II–induced cardiac dysfunction in mice. Hematoxylin-eosin staining of heart tissues showed that both celastrol and S3I attenuated Ang II–induced histopathologic alterations and cardiomyocyte hypertrophy (Figure 6A and 6B; Figure XIE in the Data Supplement). The prevention of Ang II–induced cardiac fibrosis by celastrol and S3I was confirmed using Masson trichrome and Sirius Red staining (Figure 6C through 6E). Western blot and real-time qPCR assays showed that celastrol and S3I reduced Ang II–induced prohypertrophic and profibrosis β-MyHC, collagen I, and TGF-β1 in mouse hearts (Figure 6F and 6G; Figure XIF through XIH in the Data Supplement). As expected, Ang II infusion also increased STAT3 phosphorylation and nuclear translocation in heart tissues, which were blocked by celastrol and S3I (Figure 6H through 6K). Furthermore, treatment of mice with celastrol alone did not produce structural or functional alterations in mice (Table 1; Figure 6). These results demonstrate that celastrol inhibited STAT3 activation in mouse hearts and prevented Ang II–induced cardiac remodeling.

We further determined whether celastrol treatment after Ang II challenge also affords protective effects or reverses cardiac damage. To achieve this goal, we initiated Ang II infusion in mice and maintain the mice under these conditions for 2 weeks. At this point, celastrol treatment was initiated and lasted for another 2 weeks. In this model (Table 2), celastrol did not alter body weights or blood pressure of mice (Figure XIIA and XIIB in the Data Supplement). Gross examination of harvested heart tissues showed hypertrophic changes in Ang II–challenged mice but not mice that received celastrol treatment (Figure XIIC in the Data Supplement). Assessment of heart weight:body weight and heart weight:tibia length ratios supported hypertrophic changes in mice challenged with Ang II (Table 2). Assessment of cardiac function indicated that celastrol administration preserved cardiac function in mice (Table 2; Figure XIID in the Data Supplement). These protective effects were seen in mice treated with celastrol despite elevated levels of cardiac Ang II (Figure XIIE in the Data Supplement). Similarly, celastrol reduced cardiomyocyte hypertrophy (Figure 7A and 7B) and fibrosis (Figure 7C through 7F) even when administered after Ang II challenge. Protein levels of MyHC, TGF-β1, and collagen were also reduced by celastrol (Figure 7G). These changes paralleled mRNA levels of cardiac remodeling genes, including *Myh7*, *Col1a1*, *Tgfb1*, *Anp*, *Bnp*, *α-SK*, and *Gata4* (Figure XIIF in the Data Supplement). Furthermore, celastrol suppressed Ang II–mediated STAT3 phosphorylation and nuclear localization (Figure 7H and 7I). Celastrol also reduced STAT3-KPNA3 interaction, which may explain reduced nuclear STAT3 levels (Figure XIIG in the Data Supplement). These results are consistent with our in vitro studies showing that celastrol reverses Ang II–induced cardiomyocyte remodeling.

Celastrol Reduces TAC-Induced Cardiac Remodeling

Our last objective was to determine whether celastrol prevents cardiac remodeling in other hypertrophic models through targeting STAT3. To test this, we performed TAC in mice. In this model, we initiated celastrol treatment 3 weeks after performing TAC. Mice were then maintained on celastrol for 3 weeks. Similar to our studies with Ang II challenge, celastrol did not alter body weights of mice (Figure XIIIA in the Data Supplement). Gross examination of heart tissues showed hypertrophic changes in TAC-challeneged mice (Figure XIIIB in the Data Supplement). Assessment of cardiac function showed that celastrol reduced dysfunction in mice following TAC (Table II in the Data Supplement; Figure XIIIC in the Data Supplement). Specifically, suppressed ejection fraction (%) and fractional shortening (%) were normalized by celastrol. Other parameters of cardiac function showed the same pattern. Histologically, cardiomyocyte hypertrophy and fibrosis were normalized by celastrol treatment (Figure XIIID through XIIII in the Data Supplement). Furthermore, mRNA (Figure XIVA in the Data Supplement) and protein (Figure XIVB in the Data Supplement) levels

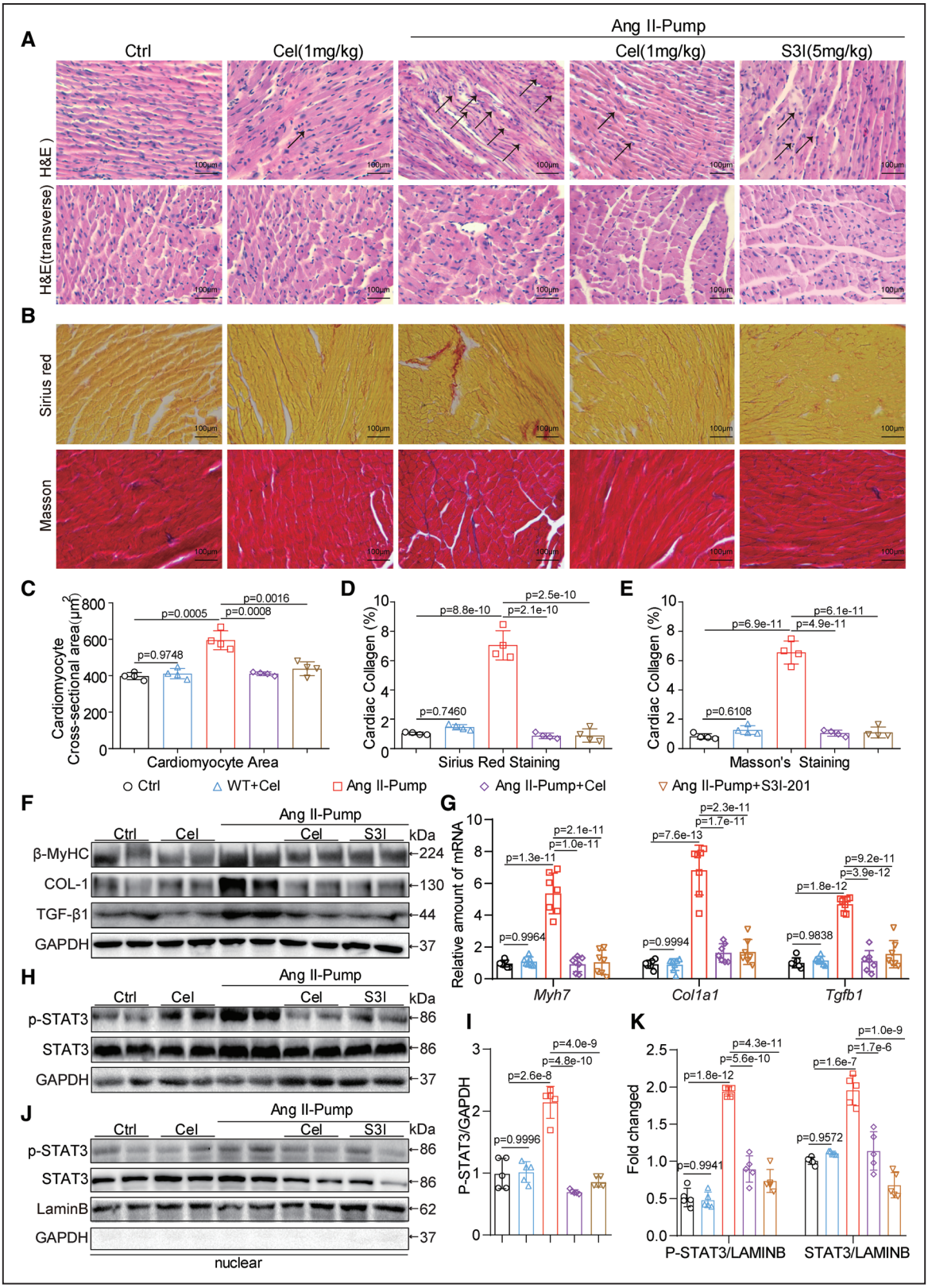

Figure 6. Celastrol prevents Ang II (angiotensin II)–induced cardiac remodeling and STAT (signal transducers and activators of transcription)-3 activation in mice with continuous Ang II infusion.

A, Representative hematoxylin-eosin staining of heart tissues showing the effect of celastrol on Ang II–induced structural deficits. Arrows indicating structural alterations. **B**, Fibrosis in heart tissues of Ang II–challenged mice. Representative micrographs of Sirius Red staining (**top**); representative micrographs of Masson trichrome staining (**bottom**). **C**, Quantitative analysis of myocyte area. A minimum of 100 cells were measured from different visual fields of 4 samples per group. **D** and **E**, Quantification of interstitial fibrotic areas (%) from Sirius (*Continued*)

Figure 6 Continued. Red–stained heart sections (**D**) and Masson trichrome staining (**E**). **F**, Representative Western blot analysis of β-MyHC (β-myosin heavy chain), collagen I, and TGF-β1 (transforming growth factor-β1) in heart tissues. GAPDH was used as loading control. **G**, Real-time quantitative polymerase chain reaction showing mRNA levels of *myh7*, *Col1a*, and *Tgfb1* in the heart tissues. **H**, Representative Western blot analysis of STAT3 and phosphotylated STAT3 (p-STAT3; Tyr-705) in heart tissues. GAPDH was used as loading control. **I**, Densitometric quantification for **H**. **J**, Representative Western blot analysis of p-STAT3 and STAT3 in nuclear extracts prepared from mouse heart tissues. Lamin B and GAPDH were used as loading control. **K**, Densitometric quantification for **J** (**C**–**K**, n=7; 1-way ANOVA followed by Tukey post hoc tests [number of comparisons, 15]. Adjusted *P* were provided in case of multiple groups).

of cardiac remodeling genes showed normalization by celastrol. Interestingly, we found that TAC induces STAT3 phosphorylation and nuclear translocation in the heart tissues (Figure XIVC and XIVD in the Data Supplement). This increased activity of STAT3 was also normalized by celastrol, consistent with our previous data from Ang II–challenged mice. Here again, the interaction between STAT3 and KPNA3 was reduced by celastrol (Figure XIVE in the Data Supplement). Collectively, these studies show that celastrol attenutes TAC-induced cardiac hypertrophy and remodeling, possibly through targeting STAT3 activation.

DISCUSSION

This study showed that celastrol provides protection against Ang II–mediated deleterious cardiac remodeling through directly binding to STAT3 protein and reducing its tyrosine phosphorylation and nuclear translocation. In mice, celastrol prevented cardiac functional deficits and reduced cardiac fibrosis and hypertrophy in both Ang II–challenged and TAC-induced mouse models. Ang II activates STAT1-3, STAT5, and STAT6 in the heart cells including myocytes.[25,40] In our study, Ang II caused a sustained phosphorylation of STAT3 in cultured cardiomyocytes and in mouse heart tissues. We also found that activated STAT3 binds to the promoter sites of *myh7*, *Col1a*, *and Tgfb1* genes and upregulates their expression. These results are consistent with indications that STAT3 is involved in myocardial hypertrophy.[25] Importantly, we show that celastrol treatment of cells prevents STAT3 phosphorylation and reduces matrix protein expression and cell size increase. Furthermore, overexpression of STAT3 reduces the protective effects of celastrol against Ang II–induced changes. In mice, we also show that celastrol mimics a selective STAT3 inhibitor in preventing functional and structural cardiac deficits induced by Ang II.

Table 2. Biometric and Echocardiographic Measurements in Experimental Mice: Model 2, in Which Celastrol was Administrated After 2-wk Ang II Challenge

	Ctrl	Continuous Ang II Pump Infusion	
			Cel (1 mg/kg)
	n=7	n=7	n=7
EF, %	79.6±1.07	73.74±2.01*	78.9±1.42#
FS, %	39.6±2.14	33.45±1.45*	38.9±1.74#
LVIDd, mm	2.1±0.48	2.4±0.85*	2.2±0.97#
IVSD, mm	0.68±0.07	0.73±0.09*	0.71±0.01^{ns}
PWd, mm	0.69±0.04	0.74±0.01*	0.70±0.03^{ns}
E wave, m/s	0.79±0.145	0.64±0.13*	0.78±0.07#
Tei Index	0.73±0.04	0.79±0.07^{ns}	0.71±0.08#
IRT, ms	19.47±0.74	24.14±0.96*	20.45±1.78^{ns}
HW/BW, mg /g	4.10±0.79	4.47+0.092*	4.13±0.089#
HW/TL, mg/mm	4.96±0.89	6.43+0.23*	5.23±0.98#

Transthoracic echocardiography was performed on mice at the end of the animal study. Data presented as mean±SEM (n=7; 1-way ANOVA followed by Tukey post hoc tests; number of comparisons, 3). Ang II indicates angiotensin II; BW, body weight; Cel, celastrol; Ctrl, control; EF ejection fraction; FS, fractional shortening; HW, heart weight; IRT, isovolumic relaxation time; IVSD, diastole interventricular septal thickness; LVIDd, diastole left ventricle internal dimension; ns, no significance; PWd, diastole posterior wall thickness; Tei index, a myocardial performance index designed by Dr Chuwa Tei; and TL, tibia length.

*$P<0.05$ compared with Ctrl.

#$P<0.05$ compared with Ang II.

Using protein microarrays, we identified STAT3 as a potential target of celastrol. Surface plasmon resonance analysis showed that celastrol binds to recombinant STAT3 protein. This interaction was further validated in ELISA and pull-down assays. It is important to note that STAT3 may not be the only target of celastrol, as celastrol appears to interact with multiple target proteins. In support of this idea, studies have shown that celastrol regulates many biological functions and signaling pathways.[41] We were careful in our interpretation and reporting of the data and elected not to overstate that STAT3 is a specific target of celastrol. Here, we have shown, for the first time to our knowledge, celastrol-binding proteins using a proteome microarray assay. Our studies indicate >100 proteins that celastrol may bind to and potentially alter. One of these proteins is STAT3. Other top interacting proteins were the Prdx. Both Prdx1 and Prdx2 prevent oxidative stress-induced cardiomyocyte apoptosis.[42,43] However, when we knocked down the expression of Prdx1 and Prdx2 in cardiomyocytes, we did not observe any changes in Ang II–induced hypertrophic and fibrotic factor expression. At least in this Ang II system, it does not appear that celastrol mediates activities through Prdx1 interaction.

An interesting question arising from our study is whether STAT3 activation leading to cardiac dysfunction is limited to Ang II challenge. STAT3 plays a different role in different heart diseases. STAT3 activation has been found to mediate cardioprotection against ischemia/reperfusion injury.[44,45] This is possibly because STAT3 activation can promote cell proliferation and prevent ischemia/reperfusion-induced cell apoptosis. Although previous reports show that STAT3 mediates Ang II–induced

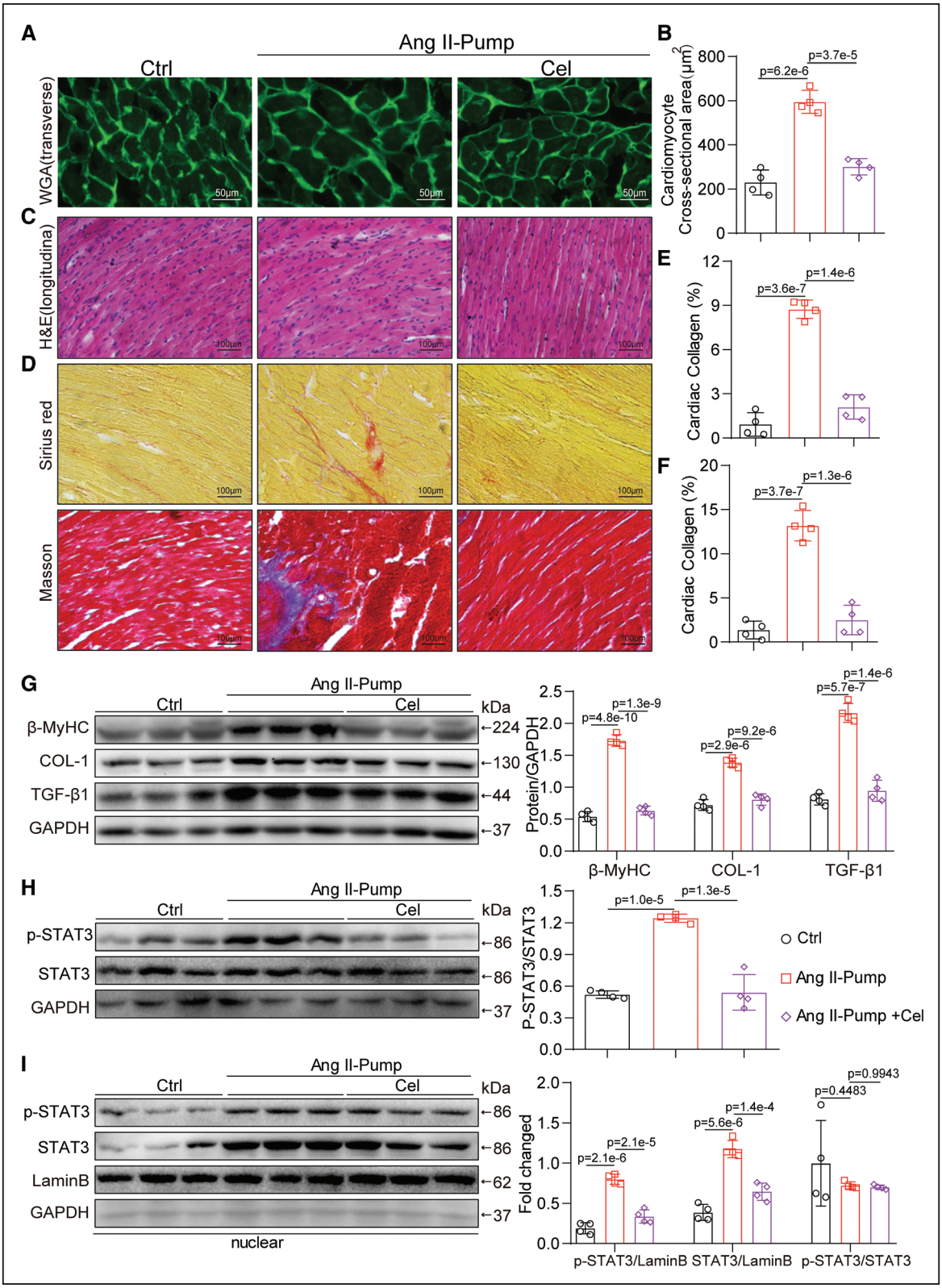

Figure 7. Celastrol reverses Ang II (angiotensin II)–induced cardiac hypertrophy and fibrosis in mice with continuous Ang II infusion.

A, Representative wheat germ agglutinin staining (WGA) staining of heart tissues showing effect of celastrol on Ang II–induced hypertrophy. **B**, Quantitative analysis of myocyte area. A minimum of 100 cells were measured from different visual fields of 4 samples per group. **C**, Representative hematoxylin-eosin staining of heart tissues showing effect of celastrol on Ang II–induced structural deficits. **D**, Fibrosis in heart tissues of Ang II–challenged mice. Representative micrographs of Sirius Red staining (**top**); representative micrographs of Masson trichrome staining (**bottom**). **E** and **F**, Quantification of interstitial fibrotic areas (%) from Sirius Red–stained heart sections (**E**) and Masson trichrome staining (**F**). (*Continued*)

Figure 7 Continued. G, Representative Western blot analysis of β-MyHC (β-myosin heavy chain), collagen I, and TGF-β1 (transforming growth factor-β1) in heart tissues. GAPDH was used as loading control. **Right**, Densitometric quantification for **G**. **H**, Representative Western blot analysis of STAT (signal transducers and activators of transcription)-3 and phosphotylated STAT3 (p-STAT3; Tyr-705) in heart tissues. GAPDH was used as loading control. **Right**, Densitometric quantification for **H**. **I**, Representative Western blot analysis of p-STAT3 and STAT3 in nuclear extracts prepared from mouse heart tissues. Lamin B and GAPDH were used as loading control. **Right**, Densitometric quantification for **I** (**A**–**I**, n=7 mice per group; **P*<0.05 compared with control; #*P*<0.05 compared with Ang II; **A**–**I**, n=1; 1-way ANOVA followed by Tukey post hoc tests [number of comparisons, 3]. Adjusted *P* values were provided in case of multiple groups).

heart injuries[46,47] and that inhibiting STAT3 reverses these injuries,[48] a few studies using gene knockout mice found that STAT3 deficiency aggravated Ang II–induced heart injuries.[49] Furthermore, cardiomyocyte-specific STAT3 deficiency also impairs cardiac contractility in hypertensive mice.[50] These discrepancies may be due to the important role of STAT3 in heart development and cardiomyogenesis.[51] Both whole-body knockout and cardiomyocyte-specific knockout of STAT3 may affect the cardiac development and function, which may aggravate the cardiac injury in Ang II or hypertensive models. Studies utilizing the selective STAT3 inhibitor S3I[39] at the onset of disease offer support for the role of abnormally activated STAT3 in cardiac dysfunction. For example, STAT3 is phosphorylated/activated in heart tissues of mice following coronary artery ligation and upon induction of diabetes mellitus.[52,53] Treatment of mice with S3I inhibits cardiac STAT3 phosphorylation in mice and prevents functional and structural alterations.[52,53] Even though we used S3I in our study as a positive control, we show that S3I reduced the levels of STAT3 phosphorylation in heart tissues of mice challenged with Ang II. These studies are certainly indirect, and it would be imperative for future studies to utilize an inducible cardiomyocyte-specific STAT3 knockout only during specific stresses to rule out developmental changes and confirm the role of STAT3 in cardiac pathology.

Other questions have also emerged from our studies. First, how does celastrol reduce Ang II–induced STAT3 phosphorylation. Marrero et al[54] have demonstrated that AT1 interacts directly with JAK2 kinase upon Ang II exposure and leads to JAK-STAT activation in vascular smooth muscle cells. Consistent with this mechanism, we show that Ang II utilized AT1 in cardiomyocytes to induce STAT3 activation, independent of β-arrestin1-ERK and PLCβ pathways. Exposure of cardiomyocytes to β-arrestin–biased or PLCβ-biased AT1 agonists also fail to induce JAK2 and STAT3 phosphorylation. We also show that celastrol does not alter Ang II–induced AT1-arrestin interaction and ERK/PLCβ phosphorylation, as well as the blood pressure in hypertensive mouse models. We further show that celastrol does not change JAK2 activation. Based on these results, together with our binding assays and docking study, celastrol appears to bind directly to STAT3 and prevent its phosphorylation.

Our studies show that celastrol is effective in reducing the levels of phospho-STAT3 when added before Ang II exposure or after. In both cases, celastrol suppressed the expression of hypertrophic and fibrotic genes. This leads to the second intriguing and emerging question as to whether suppression of STAT3 phosphorylation and nuclear translocation by celastrol are linked or mediated through distinct mechanisms. Although further studies are needed to dissect these mechanisms via celastrol-STAT3 complex crystal structural biology, our results showing reduced association between STAT3 and importin proteins upon celastrol treatment suggest a dual inhibitory mechanism of celastrol action. These dual activities may be mediated by binding of celastrol to SH2 and CCD domains of STAT3.

Collectively, our studies provide evidence that celastrol, by inhibiting STAT3, prevents Ang II–associated cardiac injury. However, its clinical application requires further research. One potential concern regarding the clinical use of celastrol currently may be the narrow therapeutic window and potential of adverse effects. Although, we have used 0.5 and 1 mg/kg in mice without any toxicity, doses reaching 3 or 4 mg/kg may produce adverse effects as has been reported recently.[55,56] Celastrol may not be utilized immediately as monotherapy for hypertension-associated cardiac remodeling, cancer, or other inflammatory conditions, but the promising results obtained in our study, as well as others, warrant further investigation. Spurred by the promising results of celastrol in various systems, researchers have started to modify celastrol to reduce its toxicity. Future studies focused on targeted release, combinatorial therapies, and chemical analogues offering favorable cellular profile would certainly help.

ARTICLE INFORMATION

Received August 15, 2019; revision received February 18, 2020; accepted February 25, 2020.

Affiliations

From the Department of Cardiology in the First Affiliated Hospital (S.Y., G.W., P.S., K.L., T.C., W.H., G.L.), Chemical Biology Research Center in School of Pharmaceutical Sciences (S.Y., W.L., Z.A.K., K.L., T.C., J.W., G.L.), and Department of Endocrinology in the First Affiliated Hospital (X.H.), Wenzhou Medical University, Zhejiang, China; and Department of Pharmacology at College of Pharmacy (the Key Laboratory of Cardiovascular Medicine Research, Ministry of Education), Harbin Medical University, Heilongjiang, China (L.X., S.W.).

Sources of Funding

This study was supported by the National Key Research Project (2017YFA0506000) and the National Natural Science Foundation of China (21961142009 to G. Liang, 81930108 to G. Liang, 81670244 to W. Huang, and 81600341 to P. Shan).

Disclosures

None.

Supplemental Materials

Expanded Materials & Methods
Online Tables I–II
Online Figures I–XIV
Major Resources Table
References[57–67]

REFERENCES

1. Metra M, Teerlink JR. Heart failure. *Lancet*. 2017;390:1981–1995. doi: 10.1016/S0140-6736(17)31071-1
2. Gradman AH, Wilson JT. Hypertension and diastolic heart failure. *Curr Cardiol Rep*. 2009;11:422–429. doi: 10.1007/s11886-009-0061-5
3. Shah SJ, Gheorghiade M. Heart failure with preserved ejection fraction: treat now by treating comorbidities. *JAMA*. 2008;300:431–433. doi: 10.1001/jama.300.4.431
4. Hamdani N, Bishu KG, von Frieling-Salewsky M, Redfield MM, Linke WA. Deranged myofilament phosphorylation and function in experimental heart failure with preserved ejection fraction. *Cardiovasc Res*. 2013;97:464–471. doi: 10.1093/cvr/cvs353
5. Kurdi M, Booz GW. New take on the role of angiotensin II in cardiac hypertrophy and fibrosis. *Hypertension*. 2011;57:1034–1038. doi: 10.1161/HYPERTENSIONAHA.111.172700
6. Valente AJ, Clark RA, Siddesha JM, Siebenlist U, Chandrasekar B. CIKS (Act1 or TRAF3IP2) mediates angiotensin-II-induced interleukin-18 expression, and Nox2-dependent cardiomyocyte hypertrophy. *J Mol Cell Cardiol*. 2012;53:113–124. doi: 10.1016/j.yjmcc.2012.04.009
7. Guo H, Liu B, Hou L, The E, Li G, Wang D, Jie Q, Che W, Wei Y. The role of mAKAPβ in the process of cardiomyocyte hypertrophy induced by angiotensin II. *Int J Mol Med*. 2015;35:1159–1168. doi: 10.3892/ijmm.2015.2119
8. Singh VP, Le B, Khode R, Baker KM, Kumar R. Intracellular angiotensin II production in diabetic rats is correlated with cardiomyocyte apoptosis, oxidative stress, and cardiac fibrosis. *Diabetes*. 2008;57:3297–3306. doi: 10.2337/db08-0805
9. Matsubara H, Moriguchi Y, Mori Y, Masaki H, Tsutsumi Y, Shibasaki Y, Uchiyama-Tanaka Y, Fujiyama S, Koyama Y, Nose-Fujiyama A, et al. Transactivation of EGF receptor induced by angiotensin II regulates fibronectin and TGF-beta gene expression via transcriptional and post-transcriptional mechanisms. *Mol Cell Biochem*. 2000;212:187–201. doi: 10.1023/a:1007189828584
10. Matsubara H, Nio Y, Murasawa S, Kijima K, Maruyama K, Mori Y, Inada M. Regulation of gene transcription of angiotensin II receptor subtypes in the heart. *Adv Exp Med Biol*. 1996;396:23–32. doi: 10.1007/978-1-4899-1376-0_3
11. McWhinney CD, Hunt RA, Conrad KM, Dostal DE, Baker KM. The type I angiotensin II receptor couples to Stat1 and Stat3 activation through Jak2 kinase in neonatal rat cardiac myocytes. *J Mol Cell Cardiol*. 1997;29:2513–2524. doi: 10.1006/jmcc.1997.0489
12. Shi J, Wei L. Regulation of JAK/STAT signalling by SOCS in the myocardium. *Cardiovasc Res*. 2012;96:345–347. doi: 10.1093/cvr/cvs321
13. Venkatesha SH, Moudgil KD. Celastrol and its role in controlling chronic diseases. *Adv Exp Med Biol*. 2016;928:267–289. doi: 10.1007/978-3-319-41334-1_12
14. Liu ZW, Wang JK, Qiu C, Guan GC, Liu XH, Li SJ, Deng ZR. Matrine pretreatment improves cardiac function in rats with diabetic cardiomyopathy via suppressing ROS/TLR-4 signaling pathway. *Acta Pharmacol Sin*. 2015;36:323–333. doi: 10.1038/aps.2014.127
15. Liu RL, Liu ZL, Li Q, Qiu ZM, Lü HJ, Yang ZM, Hong GC. [The experimental study on the inhibitory effect of tripterine on airway inflammation in asthmatic mice]. *Zhonghua Jie He He Hu Xi Za Zhi*. 2004;27:165–168.
16. Cheng M, Wu G, Song Y, Wang L, Tu L, Zhang L, Zhang C. Celastrol-induced suppression of the MiR-21/ERK signalling pathway attenuates cardiac fibrosis and dysfunction. *Cell Physiol Biochem*. 2016;38:1928–1938. doi: 10.1159/000445554
17. Der Sarkissian S, Cailhier JF, Borie M, Stevens LM, Gaboury L, Mansour S, Hamet P, Noiseux N. Celastrol protects ischaemic myocardium through a heat shock response with up-regulation of haeme oxygenase-1. *Br J Pharmacol*. 2014;171:5265–5279. doi: 10.1111/bph.12838
18. Schiaffino S, Samuel JL, Sassoon D, Lompré AM, Garner I, Marotte F, Buckingham M, Rappaport L, Schwartz K. Nonsynchronous accumulation of alpha-skeletal actin and beta-myosin heavy chain mRNAs during early stages of pressure-overload–induced cardiac hypertrophy demonstrated by in situ hybridization. *Circ Res*. 1989;64:937–948. doi: 10.1161/01.res.64.5.937
19. Perkins A, Nelson KJ, Parsonage D, Poole LB, Karplus PA. Peroxiredoxins: guardians against oxidative stress and modulators of peroxide signaling. *Trends Biochem Sci*. 2015;40:435–445. doi: 10.1016/j.tibs.2015.05.001
20. Rhee SG, Kang SW, Chang TS, Jeong W, Kim K. Peroxiredoxin, a novel family of peroxidases. *IUBMB Life*. 2001;52:35–41. doi: 10.1080/15216540252774748
21. Lohi O, Poussu A, Mao Y, Quiocho F, Lehto VP. VHS domain – a longshoreman of vesicle lines. *FEBS Lett*. 2002;513:19–23. doi: 10.1016/s0014-5793(01)03287-2
22. Wang T, Liu NS, Seet LF, Hong W. The emerging role of VHS domain-containing Tom1, Tom1L1 and Tom1L2 in membrane trafficking. *Traffic*. 2010;11:1119–1128. doi: 10.1111/j.1600-0854.2010.01098.x
23. Haghikia A, Stapel B, Hoch M, Hilfiker-Kleiner D. STAT3 and cardiac remodeling. *Heart Fail Rev*. 2011;16:35–47. doi: 10.1007/s10741-010-9170-x
24. Zouein FA, Altara R, Chen Q, Lesnefsky EJ, Kurdi M, Booz GW. Pivotal importance of STAT3 in protecting the heart from acute and chronic stress: new advancement and unresolved issues. *Front Cardiovasc Med*. 2015;2:36. doi: 10.3389/fcvm.2015.00036
25. Mascareno E, Siddiqui MA. The role of Jak/STAT signaling in heart tissue renin-angiotensin system. *Mol Cell Biochem*. 2000;212:171–175.
26. Wincewicz A, Sulkowski S. Stat proteins as intracellular regulators of resistance to myocardial injury in the context of cardiac remodeling and targeting for therapy. *Adv Clin Exp Med*. 2017;26:703–708. doi: 10.17219/acem/62693
27. Song H, Wang R, Wang S, Lin J. A low-molecular-weight compound discovered through virtual database screening inhibits Stat3 function in breast cancer cells. *Proc Natl Acad Sci USA*. 2005;102:4700–4705. doi: 10.1073/pnas.0409894102
28. Singh R. Jak2-independent activation of Stat3 by intracellular angiotensin II in human mesangial cells. *J Signal Transduct*. 2011;2011:257862. doi: 10.1155/2011/257862
29. Beak JY, Kang HS, Huang W, Myers PH, Bowles DE, Jetten AM, Jensen BC. The nuclear receptor RORα protects against angiotensin II-induced cardiac hypertrophy and heart failure. *Am J Physiol Heart Circ Physiol*. 2019;316:H186–H200. doi: 10.1152/ajpheart.00531.2018
30. Aggarwal BB, Kunnumakkara AB, Harikumar KB, Gupta SR, Tharakan ST, Koca C, Dey S, Sung B. Signal transducer and activator of transcription-3, inflammation, and cancer: how intimate is the relationship? *Ann N Y Acad Sci*. 2009;1171:59–76. doi: 10.1111/j.1749-6632.2009.04911.x
31. Zhong Z, Wen Z, Darnell JE Jr. Stat3: a STAT family member activated by tyrosine phosphorylation in response to epidermal growth factor and interleukin-6. *Science*. 1994;264:95–98. doi: 10.1126/science.8140422
32. Liu L, McBride KM, Reich NC. STAT3 nuclear import is independent of tyrosine phosphorylation and mediated by importin-alpha3. *Proc Natl Acad Sci USA*. 2005;102:8150–8155. doi: 10.1073/pnas.0501643102
33. Reich NC, Liu L. Tracking STAT nuclear traffic. *Nat Rev Immunol*. 2006;6:602–612. doi: 10.1038/nri1885
34. Ikeda Y, Kumagai H, Motozawa Y, Suzuki J, Komuro I. Biased agonism of the angiotensin II type I receptor. *Int Heart J*. 2015;56:485–488. doi: 10.1536/ihj.15-256
35. Wingler LM, McMahon C, Staus DP, Lefkowitz RJ, Kruse AC. Distinctive activation mechanism for angiotensin receptor revealed by a synthetic nanobody. *Cell*. 2019;176:479–490.e12. doi: 10.1016/j.cell.2018.12.006
36. Regan JA, Mauro AG, Carbone S, Marchetti C, Gill R, Mezzaroma E, Valle Raleigh J, Salloum FN, Van Tassell BW, Abbate A, et al. A mouse model of heart failure with preserved ejection fraction due to chronic infusion of a low subpressor dose of angiotensin II. *Am J Physiol Heart Circ Physiol*. 2015;309:H771–H778. doi: 10.1152/ajpheart.00282.2015
37. Wang L, Zhang YL, Lin QY, Liu Y, Guan XM, Ma XL, Cao HJ, Liu Y, Bai J, Xia YL, et al. CXCL1-CXCR2 axis mediates angiotensin II-induced cardiac hypertrophy and remodelling through regulation of monocyte infiltration. *Eur Heart J*. 2018;39:1818–1831. doi: 10.1093/eurheartj/ehy085
38. Yang K, Zhang TP, Tian C, Jia LX, Du J, Li HH. Carboxyl terminus of heat shock protein 70-interacting protein inhibits angiotensin II-induced cardiac remodeling. *Am J Hypertens*. 2012;25:994–1001. doi: 10.1038/ajh.2012.74
39. Siddiquee K, Zhang S, Guida WC, Blaskovich MA, Greedy B, Lawrence HR, Yip ML, Jove R, McLaughlin MM, Lawrence NJ, et al. Selective chemical probe inhibitor of Stat3, identified through structure-based virtual screening, induces antitumor activity. *Proc Natl Acad Sci USA*. 2007;104:7391–7396. doi: 10.1073/pnas.0609757104
40. Kodama H, Fukuda K, Pan J, Makino S, Sano M, Takahashi T, Hori S, Ogawa S. Biphasic activation of the JAK/STAT pathway by angiotensin II in rat cardiomyocytes. *Circ Res*. 1998;82:244–250. doi: 10.1161/01.res.82.2.244

41. Ng SW, Chan Y, Chellappan DK, Madheswaran T, Zeeshan F, Chan YL, Collet T, Gupta G, Oliver BG, Wark P, et al. Molecular modulators of celastrol as the keystones for its diverse pharmacological activities. *Biomed Pharmacother*. 2019;109:1785–1792. doi: 10.1016/j.biopha.2018.11.051
42. Guo W, Liu X, Li J, Shen Y, Zhou Z, Wang M, Xie Y, Feng X, Wang L, Wu X. Prdx1 alleviates cardiomyocyte apoptosis through ROS-activated MAPK pathway during myocardial ischemia/reperfusion injury. *Int J Biol Macromol*. 2018;112:608–615. doi: 10.1016/j.ijbiomac.2018.02.009
43. Zhao W, Fan GC, Zhang ZG, Bandyopadhyay A, Zhou X, Kranias EG. Protection of peroxiredoxin II on oxidative stress-induced cardiomyocyte death and apoptosis. *Basic Res Cardiol*. 2009;104:377–389. doi: 10.1007/s00395-008-0764-6
44. Negoro S, Kunisada K, Fujio Y, Funamoto M, Darville MI, Eizirik DL, Osugi T, Izumi M, Oshima Y, Nakaoka Y, et al. Activation of signal transducer and activator of transcription 3 protects cardiomyocytes from hypoxia/reoxygenation-induced oxidative stress through the upregulation of manganese superoxide dismutase. *Circulation*. 2001;104:979–981. doi: 10.1161/hc3401.095947
45. Oshima Y, Fujio Y, Nakanishi T, Itoh N, Yamamoto Y, Negoro S, Tanaka K, Kishimoto T, Kawase I, Azuma J. STAT3 mediates cardioprotection against ischemia/reperfusion injury through metallothionein induction in the heart. *Cardiovasc Res*. 2005;65:428–435. doi: 10.1016/j.cardiores.2004.10.021
46. Tsai CT, Lai LP, Kuo KT, Hwang JJ, Hsieh CS, Hsu KL, Tseng CD, Tseng YZ, Chiang FT, Lin JL. Angiotensin II activates signal transducer and activators of transcription 3 via Rac1 in atrial myocytes and fibroblasts: implication for the therapeutic effect of statin in atrial structural remodeling. *Circulation*. 2008;117:344–355. doi: 10.1161/CIRCULATIONAHA.107.695346
47. Xue XD, Huang JH, Wang HS. Angiotensin II activates signal transducers and activators of transcription 3 via Rac1 in the atrial tissue in permanent atrial fibrillation patients with rheumatic heart disease. *Cell Biochem Biophys*. 2015;71:205–213. doi: 10.1007/s12013-014-0186-z
48. Skoumal R, Tóth M, Serpi R, Rysä J, Leskinen H, Ulvila J, Saiho T, Aro J, Ruskoaho H, Szokodi I, et al. Parthenolide inhibits STAT3 signaling and attenuates angiotensin II-induced left ventricular hypertrophy via modulation of fibroblast activity. *J Mol Cell Cardiol*. 2011;50:634–641. doi: 10.1016/j.yjmcc.2011.01.001
49. Zouein FA, Zgheib C, Hamza S, Fuseler JW, Hall JE, Soljancic A, Lopez-Ruiz A, Kurdi M, Booz GW. Role of STAT3 in angiotensin II-induced hypertension and cardiac remodeling revealed by mice lacking STAT3 serine 727 phosphorylation. *Hypertens Res*. 2013;36:496–503. doi: 10.1038/hr.2012.223
50. Altara R, Harmancey R, Didion SP, Booz GW, Zouein FA. Cardiac STAT3 deficiency impairs contractility and metabolic homeostasis in hypertension. *Front Pharmacol*. 2016;7:436. doi: 10.3389/fphar.2016.00436
51. Foshay K, Rodriguez G, Hoel B, Narayan J, Gallicano GI. JAK2/STAT3 directs cardiomyogenesis within murine embryonic stem cells in vitro. *Stem Cells*. 2005;23:530–543. doi: 10.1634/stemcells.2004-0293
52. Tang TT, Li YY, Li JJ, Wang K, Han Y, Dong WY, Zhu ZF, Xia N, Nie SF, Zhang M, et al. Liver-heart crosstalk controls IL-22 activity in cardiac protection after myocardial infarction. *Theranostics*. 2018;8:4552–4562. doi: 10.7150/thno.24723
53. Chen Y, Surinkaew S, Naud P, Qi XY, Gillis MA, Shi YF, Tardif JC, Dobrev D, Nattel S. JAK-STAT signalling and the atrial fibrillation promoting fibrotic substrate. *Cardiovasc Res*. 2017;113:310–320. doi: 10.1093/cvr/cvx004
54. Marrero MB, Schieffer B, Paxton WG, Heerdt L, Berk BC, Delafontaine P, Bernstein KE. Direct stimulation of Jak/STAT pathway by the angiotensin II AT1 receptor. *Nature*. 1995;375:247–250. doi: 10.1038/375247a0
55. Konieczny J, Jantas D, Lenda T, Domin H, Czarnecka A, Kuter K, Śmiałowska M, Lasoń W, Lorenc-Koci E. Lack of neuroprotective effect of celastrol under conditions of proteasome inhibition by lactacystin in in vitro and in vivo studies: implications for Parkinson's disease. *Neurotox Res*. 2014;26:255–273. doi: 10.1007/s12640-014-9477-9
56. Li HY, Zhang J, Sun LL, Li BH, Gao HL, Xie T, Zhang N, Ye ZM. Celastrol induces apoptosis and autophagy via the ROS/JNK signaling pathway in human osteosarcoma cells: an in vitro and in vivo study. *Cell Death Dis*. 2015;6:e1604. doi: 10.1038/cddis.2014.543
57. Zhang HN, Yang L, Ling JY, Czajkowsky DM, Wang JF, Zhang XW, Zhou YM, Ge F, Yang MK, Xiong Q, et al. Systematic identification of arsenic-binding proteins reveals that hexokinase-2 is inhibited by arsenic. *Proc Natl Acad Sci USA*. 2015;112:15084–15089. doi: 10.1073/pnas.1521316112
58. Huang da W, Sherman BT, Lempicki RA. Systematic and integrative analysis of large gene lists using DAVID bioinformatics resources. *Nat Protoc*. 2009;4:44–57. doi: 10.1038/nprot.2008.211
59. Huang da W, Sherman BT, Lempicki RA. Bioinformatics enrichment tools: paths toward the comprehensive functional analysis of large gene lists. *Nucleic Acids Res*. 2009;37:1–13. doi: 10.1093/nar/gkn923
60. Morris GM, Huey R, Lindstrom W, Sanner MF, Belew RK, Goodsell DS, Olson AJ. AutoDock4 and AutoDockTools4: automated docking with selective receptor flexibility. *J Comput Chem*. 2009;30:2785–2791. doi: 10.1002/jcc.21256
61. Salomon-Ferrer R, Case RA, Walker RC. An overview of the amber biomolecular simulation package. *WIREs Computational Molecular Science*. 2012;3:198–210.
62. Chen J, Lai J, Yang L, Ruan G, Chaugai S, Ning Q, Chen C, Wang DW. Trimetazidine prevents macrophage-mediated septic myocardial dysfunction via activation of the histone deacetylase sirtuin 1. *Br J Pharmacol*. 2016;173:545–561. doi: 10.1111/bph.13386
63. Ortiz-Sánchez P, Villalba-Orero M, López-Olañeta MM, Larrasa-Alonso J, Sánchez-Cabo F, Martí-Gómez C, Camafeita E, Gómez-Salinero JM, Ramos-Hernández L, Nielsen PJ, et al. Loss of SRSF3 in cardiomyocytes leads to decapping of contraction-related mRNAs and severe systolic dysfunction. *Circ Res*. 2019;125:170–183. doi: 10.1161/CIRCRESAHA.118.314515
64. McGrath JC, Drummond GB, McLachlan EM, Kilkenny C, Wainwright CL. Guidelines for reporting experiments involving animals: the ARRIVE guidelines. *Br J Pharmacol*. 2010;160:1573–1576. doi: 10.1111/j.1476-5381.2010.00873.x
65. Chakraborty D, Šumová B, Mallano T, Chen CW, Distler A, Bergmann C, Ludolph I, Horch RE, Gelse K, Ramming A, et al. Activation of STAT3 integrates common profibrotic pathways to promote fibroblast activation and tissue fibrosis. *Nat Commun*. 2017;8:1130. doi: 10.1038/s41467-017-01236-6
66. Kandalam V, Basu R, Abraham T, Wang X, Soloway PD, Jaworski DM, Oudit GY, Kassiri Z. TIMP2 deficiency accelerates adverse post-myocardial infarction remodeling because of enhanced MT1-MMP activity despite lack of MMP2 activation. *Circ Res*. 2010;106:796–808. doi: 10.1161/CIRCRESAHA.109.209189
67. Xue K, Zhang J, Li C, Li J, Wang C, Zhang Q, Chen X, Yu X, Sun L, Yu X. The role and mechanism of transforming growth factor beta 3 in human myocardial infarction-induced myocardial fibrosis. *J Cell Mol Med*. 2019;23:4229–4243. doi: 10.1111/jcmm.14313